Spatial Structure of Zervamicin IIB Bound to DPC Micelles: Implications for Voltage-Gating

Z. O. Shenkarev,* T. A. Balashova,* R. G. Efremov,* Z. A. Yakimenko,* T. V. Ovchinnikova,* J. Raap,† and A. S. Arseniev*

*Shemyakin-Ovchinnikov Institute of Bioorganic Chemistry, Russian Academy of Sciences, 117997 Moscow, Russia, and †Leiden Institute of Chemistry, Gorlaeus Laboratories, Leiden University, 2300 RA, Leiden, The Netherlands

ABSTRACT Zervamicin IIB is a 16-amino acid peptaibol that forms voltage-dependent ion channels with multilevel conductance states in planar lipid bilayers and vesicular systems. The spatial structure of zervamicin IIB bound to dodecylphosphocholine micelles was studied by nuclear magnetic resonance spectroscopy. The set of 20 structures obtained has a bent helical conformation with a mean backbone root mean square deviation value of ~0.2 Å and resembles the structure in isotropic solvents (Balashova et al., 2000. NMR structure of the channel-former zervamicin IIB in isotropic solvents. *FEBS Lett* 466:333–336). The *N*-terminus represents an α-helix, whereas the *C*-terminal part has a mixed $3_{10}/\alpha_R$ hydrogen-bond pattern. In the anisotropic micelle environment, the bending angle on Hyp10 (23°) is smaller than that (47°) in isotropic solvents. In the NOESY (Nuclear Overhauser Effect Spectroscopy) spectra, the characteristic attenuation of the peptide signals by 5- and 16-doxylstearate relaxation probes indicates a peripheral mode of the peptaibol binding to the micelle with the *N*-terminus immersed slightly deeper into micelle interior. Analysis of the surface hydrophobicity reveals that the zervamicin IIB helix is amphiphilic and well suited to formation of a tetrameric transmembrane bundle, according to the barrel-stave mechanism. The results are discussed in a context of voltage-driven peptaibol insertion into membrane.

INTRODUCTION

Peptide antibiotics forming amphiphilic helices in the presence of lipid bilayers play an important role in defense systems of various organisms. There is a variety of subtypes of such antibiotics produced by fungi, insects, amphibia, and mammalians. The mechanism of action of these agents remains unclear, although studies of their activity on model systems suggest that the peptides interact with the membrane of the target cell. The antibiotic property is thought to be related to the increased ion permeability of the membrane (Bechinger, 1999; Epand and Vogel, 1999). With the expansion of pathogenic organisms resistant to conventional antibiotics, the pharmacological application of antimicrobial peptides attracts steadily increasing interest (Gabay, 1994).

The object of our study zervamicin-IIB (Zrv-IIB) is a member of the antibiotic peptaibol-family. Peptaibols are small (7–24 amino acids) peptides of fungal origin, which contain a high proportion of helix-promoting α, α-dialkylated amino acids (Aib, α-aminoisobutyric acid; Iva, D-isovaline), an acetylated *N*-terminus and a *C*-terminal α-amino alcohol (Sansom, 1991). Zrv-IIB and several other highly homologous zervamicins were isolated from cultures of *Emericellopsis salmosynnemata* (Argoudelis et al., 1974). Zervamicins consist of 16 amino acid residues. The sequence of Zrv-IIB is:

AcTrp-Ile-Gln-Iva-Ile^5-Thr-Aib-Leu-Aib-Hyp^{10}-Gln-Aib-Hyp-Aib-Pro-Phl^{16} (Hyp, 4-hydroxyproline; Phl, L-phenylalaninol).

In zervamicins the characteristic Gly^{11}-x-x-Pro^{14} motif of the alamethicin-peptaibol subfamily is replaced by Aib^7-x-x-Hyp^{10} (Sansom, 1991).

Zrv-IIB is active against Gram-positive bacteria, less active against Gram-negative bacteria, and nontoxic for eukaryotic cells (Argoudelis et al., 1974; Argoudelis and Johnson, 1975). In planar lipid bilayers (Balaram et al., 1992) and vesicular systems (Kropacheva and Raap, 1999), Zrv-IIB forms voltage-dependent ion channels with multilevel conductance states. The current-voltage relationships for Zrv-IIB are very asymmetric. The peptide forms channels in the presence of *cis*-positive potentials only (*cis* denotes the side of bilayer to which the peptide was added), although at high peptide concentrations, it demonstrates potential-independent behavior (Kropacheva and Raap, 1999).

The conventional model for voltage-gated peptaibol action (the so-called barrel-stave (BS) model) (Baumann and Mueller, 1974; Sansom, 1991) involves the formation of an electrolyte-filled pore by a bundle of parallel helices. It is generally thought that different conductance levels correspond to different helix bundles. The transitions between levels occur only in a sequential manner by the release or uptake of the monomers from the conducting aggregate. It is worth noting that the BS model is generally accepted to describe naturally occurring ion channels (Marsh, 1996) and, hence, peptaibols can be considered more realistic models of the voltage-gated channels than gramicidin and other channel-forming peptides (Sansom, 1998).

Submitted May 21, 2001 and accepted for publication October 12, 2001.

Address reprint requests to: A. S. Arseniev, Shemyakin-Ovchinnikov Institute of Bioorganic Chemistry, Russian Academy of Sciences, ul. Miklukho-Maklaya, 16/10, 117997 Moscow, Russia. Tel.: 7-095-3305929; Fax: 7-095-3355033; E-mail: aars@nmr.ru.

0006-3495/02/02/762/10 $2.00

The BS model corresponds well to the experimental data on multistates' conductance levels and voltage-current asymmetry, but the mechanism of the peptaibol voltage-gating remains unclear. The models for voltage-gated peptaibol channels, initially proposed for alamethicin, involve either voltage-driven conformational changes in the transmembrane bundle of the petaibol molecules (bending around Pro^{14} (Fox and Richards, 1982), or around the residues Aib^{10}, Gly^{11}, Leu^{12} (Franklin et al., 1994; Yee et al., 1995)) or voltage-driven insertion into the membrane of molecular helical dipoles.

The relatively small size of antimicrobial peptides make them ideal objects for nuclear magnetic resonance (NMR) investigation (Bechinger, 1999; Epand and Vogel, 1999). In our previous work (Balashova et al., 2000) the spatial structure of Zrv-IIB was determined in isotropic solvents. It was shown that in solvents of different polarity (ranging from chloroform/methanol (9:1 v/v) to methanol/water (1:1 v/v)) the peptide maintains a well defined spatial structure. These results suggest that the voltage gating of Zrv-IIB is not conditioned by substantial conformational changes.

The large size of the membrane-peptide system makes it difficult to determine the spatial structure of a membrane-bound peptide in its native environment. Therefore, membrane mimetics, such as detergent micelles, are commonly used in NMR studies of membrane peptides and proteins (Opella et al., 1994; Henry and Sykes, 1994; Pervushin and Arseniev, 1995). Although the micelles do not exactly reproduce the membrane environment (they possess a highly curved surface in contrast to flat bilayers), in some cases they are able to maintain the spatial structure and functionality of transmembrane (TM) peptides and proteins (Pervushin and Arseniev, 1995; Vinogradova et al., 1998).

Here we report the spatial structure of Zrv-IIB incorporated into dodecylphosphocholine (DPC) micelles. Using lipid-soluble paramagnetic spin labels, we show that the peptide is bound to the micelle surface and oriented approximately parallel to it. Comparison with the previous study shows that the spatial structure of Zrv-IIB changes only slightly upon transition from isotropic solvents of different polarity to the heterogeneous micellar environment. These results provide further evidence for the insertion model of voltage gating.

MATERIALS AND METHODS

Sample preparation

Zrv-IIB was isolated and purified according to the previously described protocol (Balashova et al., 2000). Nondeuterated DPC and its perdeuterated analog (98% deuterium) were purchased from Avanti Polar Lipids (Alabaster, AL). The 5- and 16-doxylstearates are products of Sigma (St. Louis, MO). D_2O (99.9% deuterium) was purchased from Isotope (Moscow, Russia).

The sample containing Zrv-IIB in micellar solution was prepared as follows. A mixture of dry DPC (16.6 mg) and dry Zrv-IIB (2 mg) was dissolved in 0.5 ml of a 1:1 mixture of 2,2,2-trifluoroethyl alcohol/chloroform. The obtained solution was evaporated in vacuum and dissolved in 0.5 ml D_2O. After that, the sample was sonicated and lyophilized. The solid residual was again dissolved in 0.5 ml D_2O and lyophilized. The last operation was repeated twice. Finally, the sample was dissolved in 0.6 ml H_2O (10% D_2O) and used in the NMR experiments. The resulting concentration of Zrv-IIB was 1.8 mM and the peptide/detergent ratio was 1:40. Unless otherwise stated, the pH of the sample was 6.8–7.0. The 5- and 16-doxylstearates were added as a solution in methanol-d4. The molar ratio of detergent to spin-label was 63:1. The maximal amount of deuterated methanol in the sample was 3 μl and the pH was controlled before and after addition of the spin probe. To measure the deuterium exchange rates of amide protons, the sample was lyophilized and dissolved in D_2O, pH 4.8 (direct pH-meter readings). The sample for diffusion measurements of DPC micelles was prepared by dissolving 16.6 mg of nondeuterated DPC in 0.6 ml H_2O (10% D_2O).

NMR spectroscopy, data processing, and spectral assignment

All NMR experiments were performed on a Varian Unity-600 spectrometer (Varian, Palo Alto, CA). DQF-COSY (Rance et al., 1983), TOCSY (Bax and Davis, 1985) with mixing times (τ_m) of 70 ms, and NOESY (Jeener et al., 1979) with τ_m values of 50, 100, and 200 ms were recorded in the pure phase-absorption mode by collecting hypercomplex data (States et al., 1982). The Watergate (Piotto et al., 1992) and Flip-back (Lippens et al., 1995) techniques were used to suppress strong solvent resonance. A relaxation delay of 3.2 s was used. Unless otherwise stated, all NMR experiments were performed at the temperature of 30°C. Chemical shifts were measured relative to the protons of H_2O, the chemical shift of the signal being arbitrarily chosen as 4.75 ppm. For the diffusion measurements, a slightly modified version of the spin-echo experiment was used (Dubovskii et al., 2001). Before the diffusion experiments, the temperature of the sample was allowed to equilibrate for at least 1 h. The calibration of the gradient unit was performed using the same method and the set of solvents as in Orekhov et al. (1999). Thirty one-dimensional (1-D) NMR spectra were recorded with the strength of the encoding/decoding pulse field gradients varied in the range from 0 to ~30 Gs/cm. Delays for the diffusion of 150–350 ms were used. A relaxation delay of 5 s was used before each scan. The signals of the well resolved protons in the 1-D spectra were used to process the diffusion data on Zrv-IIB/DPC complexes or nondeuterated DPC. Self-diffusion rates and their uncertainties were obtained by the two-parameter least-squares exponential fit to the signal decays versus the square of the gradient strength.

To detect amide protons with slow hydrogen deuterium exchange rates, 1-D and 2-D NOESY spectra were recorded in a 4-h repetition cycle starting after dissolution of the Zrv-IIB/DPC sample in D_2O, pH 4.8, 30°C. The rates of amide protons exchange on the solvent deuterons were determined by the exponential fitting of the measured peak intensities of the 1-D spectra or in the fingerprint region of the NOESY spectra. Temperature coefficients of the chemical shifts of the amide protons were measured by linear fitting of the chemical shift values determined from the 1-D and 2-D NOESY spectra recorded in the temperature range from 15 to 50°C.

All NMR spectra were processed and quantified using macros within the VNMR software (Varian). For further analysis 2-D spectra were converted into the format of the XEASY program (Bartels et al., 1995). Proton resonance assignments for L-amino acids were obtained by a standard procedure (Wuthrich, 1986); assignment of Aib and Iva residues was performed simultaneously with the sequential assignment. Crosspeak intensities were measured using an algorithm of a nonlinear least-squares approximation for lineshapes of the crosspeak sections in both directions of the 2-D spectra implemented in the XEASY program. $^3J_{N\alpha}$ coupling constants were determined with the program INFIT (Szyperski et al., 1992) from the NOESY crosspeaks. $^3J_{\alpha\beta}$ coupling constants were evaluated by

the analysis of patterns of α/β crosspeaks in the DQF-COSY spectrum of the Zrv-IIB/DPC sample in D_2O.

Experimental constraints and spatial structure calculation

The spatial structure calculation was performed using the simulated annealing/molecular dynamics protocol as implemented in the DYANA program version 1.5 (Guntert et al., 1997). Interproton distance constraints were derived from the crosspeak intensities measured in the NOESY spectra with $\tau_m = 100$ ms, where spin-diffusion effects might be ignored. Meaningful interproton distance constraints (174) were derived from 536 unambiguously assigned NOESY crosspeak volumes via a $1/r^6$ calibration with the CALIBA function of DYANA.

Stereospecific assignments of β-methylene protons and torsion angle constraints for χ^1 angles of amino acids were obtained by analysis of the local structure in the HABAS function of DYANA using the available $^3J_{\alpha\beta}$ spin-spin coupling constants and NOE distance constraints derived from the NOESY spectrum with $\tau_m = 50$ ms. Pseudoatom constraints were used in cases when the stereospecific assignment for prochiral centers was unknown. The side chains of Zrv-IIB are often mobile, and the crosspeaks arising from their protons correspond to a set of conformations. To eliminate unrealistic conformations and to describe the available conformational space, we did not constrain those protons nor pseudocenters that were affected by the angles for which we could not reject their mobility. Application of the procedure (Dementieva et al., 1999) gives torsion angle constraints and stereospecific assignments. Stereospecific assignments of β, γ, δ-methylene protons for imino acids (Pro/Hyp) were obtained based on NOESY crosspeak volumes in spectrum with $\tau_m = 50$ ms.

Stereospecific assignments of β-methyl groups for Aib residues and helix handedness in the *C*-terminus were determined using iterative cycles of structure calculation. On each stage, assignment of one Aib residue was changed. The analysis of corresponding changes in the DYANA target function led to the assignment of all eight methyl groups. The calculations revealed that only a right-handed conformation is compatible with the experimental data. Based on this information, eight torsion angle constraints for the φ angles were derived from $^3J_{N\alpha}$ spin-spin coupling constants in HABAS function of the DYANA.

After generation of the set of 50 structures matching the interproton upper distance and torsion angle constraints, 29 additional lower distance constraints (3.0 Å), based on the expected crosspeaks (according to the structures obtained) but not present in the NOESY spectra with $\tau_m = 200$ ms, were introduced as described in Jaravine et al. (1997).

Ten amide protons which have a half-exchange time to solvent deuterons >1 h and temperature coefficients of the chemical shifts <6 ppb/°C were supposed to be involved in hydrogen bonds. The acceptors of hydrogen bonds were found by the analysis of preliminary structures (the hydrogen bonds were observed in >30 of 50 calculated structures). In accordance with geometric criteria for hydrogen bonds (Baker and Hubbard, 1984), six distance constraints were used in subsequent calculation for each hydrogen bond: three upper (3.3, 2.3, 3.5 Å) and three lower (2.5, 1.8, 2.6 Å) for $i + 4 \rightarrow i$ hydrogen bonds (α-helix), as well as three upper (3.4, 2.4, 3.5 Å) and three lower (2.6, 1.9, 2.2 Å) for $i + 3 \rightarrow i$ hydrogen bonds (3_{10}-helix) for d(O, N), d(O, H^N), and d(C, H^N) distances, respectively.

The next generation of 100 structures was calculated with the addition of hydrogen bonds and lower distance constraints, and the best 20 of them were selected according to the following criteria: (1) each structure differs from all others by a root mean square deviation (rmsd) of the backbone atom coordinates $\geq$0.05 Å and (2) a low final DYANA target function ($\leq$0.02 Å^2). To prevent bad sterical contacts, the best 20 DYANA structures were subjected to the conjugate gradients energy minimization in the program Discover (Insight II (2.1.0), Biosym Technologies, San Diego, CA) with the CVFF (consistent valence force field) (Dauber-Osguthorpe et al., 1988) and the same distance and torsion angle restraints, as used on the last stage of the DYANA's protocol. This resulted in a remarkable decreasing of van der Waals forces and restraint terms in the total energy, although the rmsd in the set of structures did not change significantly.

Visual analysis of the structures and figure drawings were performed using the MOLMOL program (Koradi et al., 1996). The molecular hydrophobicity potential (MHP) created by peptide atoms in the surface points of the lowest-energy helical structure of Zrv-IIB was calculated as described in Efremov and Vergoten (1995). The resulting distribution of the MHP was visualized by means of 2-D isopotential plots of the α and z coordinates, where α is the rotation angle around the helix axis, and z is the rise distance along the helix axis.

Protein Data Bank and BioMagnetic Resonance Bank accession codes

The chemical shifts of Zrv-IIB in the presence of DPC micelles have been deposited into the BioMagnetic Resonance Bank (accession code 4993). NMR constraints and derived atomic coordinates (20 models) have been deposited into the Protein Data Bank (accession code 1IH9).

RESULTS

Stoichiometry of the Zrv-IIB/DPC micelle complex

Like many other peptaibols, Zrv-IIB itself is not water-soluble and, according to our assumption, in the presence of DPC, all peptide molecules are in the micelle-bound form. We monitored the complex formation between DPC and Zrv-IIB via diffusion measurements at 30°C of pure DPC micelles and mixed DPC/Zrv-IIB micelles. Measured diffusion constants ($1.20 \pm 0.02 \times 10^{-10}$ m^2/s pure DPC; $1.06 \pm 0.02 \times 10^{-10}$ m^2/s Zrv-IIB/DPC complex) and corresponding hydrodynamic Stokes radii (23.1 $\pm$ 0.5 Å; 26.2 $\pm$ 0.5 Å) revealed that the size of micelles is slightly altered by the Zrv-IIB binding. Ultracentrifugation, light scattering (Lauterwein et al., 1979), and electronic paramagnetic resonance (EPR) (Brown et al., 1981) studies have shown that DPC at concentrations used in NMR experiments forms uniformly sized micelles comprised of 50–60 detergent molecules. At the experimental conditions (70 mM DPC; peptide:detergent ratio 1:40) used here, no evidence was found for Zrv-IIB aggregation. We estimated the aggregation number for Zrv-IIB/DPC complex, based on the assumptions that the peptide is monomeric and evenly distributed between DPC micelles and that the density of micelle is not changed upon Zrv-IIB binding. This calculation shows that ~1.6 ($\pm$ 0.3) peptaibol molecules are bound per one micelle consisting of ~66 ($\pm$ 12) molecules of detergent.

NMR assignments

Spin systems of all L-amino acids were identified in the DQF-COSY and TOCSY spectra. The aromatic spin systems of Trp[1] and Phl[16] were assigned on the basis of the NOE connectivities between aliphatic and aromatic protons.

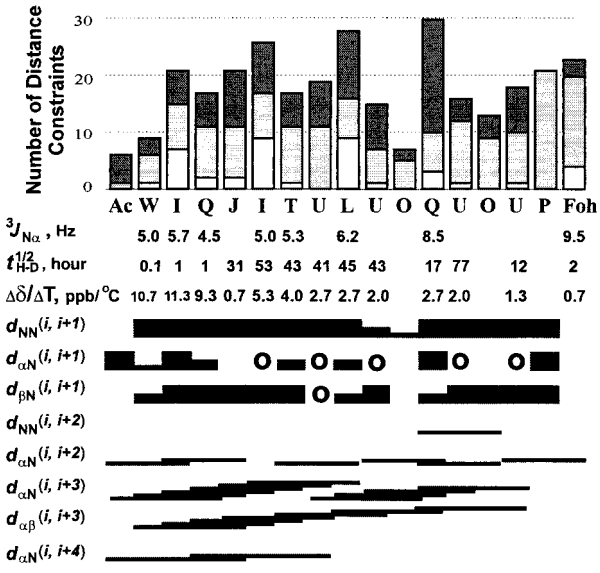

FIGURE 1 Overview of the NMR data collected for 1.8 mM Zrv-IIB in 72 mM DPC at pH 6.8 and 30°C. The amino acid sequence is given in the one letter code, where acetyl, Aib (α-aminoisobutyric acid), Iva (D-isovaline), Hyp (4-hydroxyproline), Phl (α-aminophenylalaninol) are abbreviated as Ac, U, J, O, and Foh, respectively, and the other residues as usual. The NOE connectivities are denoted as usual: d_{AB} (i, j) is the connectivity between the proton types A and B located in amino acid residues i and j, respectively. N, α, and β denote amide ($C^{\delta}H_2$ for O^{10}, O^{13}, and P^{15} residues), H^{α} (C^{α}-CH_3 for J^4, U^7, U^9, U^{12}, and U^{14} residues), and H^{β} protons, respectively. Lines, half- and full-size squares denote low, medium, and high intensity of corresponding crosspeaks in the NOESY 100 ms spectrum, respectively. The circle indicates overlapping crosspeaks. The number of distance constraints, used in the structure calculation, is shown at the top of the figure. White, light-gray, and black rectangles correspond to intraresidue, sequential, and medium-range ($1 < i - j \leq 4$) constraints, respectively. Values of $^3J_{N\alpha}$ coupling constants, temperature coefficients of chemical shifts of amide proton signals ($\Delta\delta/\Delta T$), and half-exchange times of amide protons with solvent deuterons ($t_{1/2HD}$, pH 4.8, 30°C) are shown in corresponding lines.

The assignment of Iva^4 resonances was obtained by analysis of the characteristic TOCSY pattern of the $C^{\beta}H_2$-$C^{\gamma}H_3$ fragment in addition to their intraresidue NOESY crosspeaks $d_{\beta N}(i, i)$. Then the sequential assignment was carried out using $d_{NN}(i, i + 1)$, $d_{\alpha N}(i, i + 1)$, and $d_{\beta N}(i, i + 1)$ connectivities (Fig. 1). In most previous NMR studies of peptaibols, it has proven difficult to obtain complete assignments for the methyl groups of the Aib residues. However, in our case this problem was significantly alleviated. Zrv-IIB contains only four Aib residues with nondegenerated chemical shifts of amide and methyl protons. Thus, assignment of all eight methyl group was easily obtained using the NOE $d_{\beta N}(i, i)$ crosspeaks.

Qualitative characterization of the Zrv-IIB conformation

A summary of the NMR data obtained for Zrv-IIB in the DPC micelles solution is shown in Fig. 1. The absence of long range (i-$j > 4$) contacts and NOE connectivities $d_{\alpha N}(i, i + 2)$ and $d_{\alpha N}(i, i + 3)$ distributed along the sequence, argues for a helical conformation of the molecule. The $^3J_{N\alpha}$ spin-spin coupling constants on the *N*-terminus are consistent with this, having the values ~5Hz, which are typical for right-handed helical conformation. Based on this data, it is difficult to discriminate between 3_{10}- and α-helices on the *N*-terminus. However, the $d_{\alpha N}(i, i + 4)$ contacts which have never been observed in 3_{10}-helices count in favor of the α-helix (Wuthrich, 1986).

In addition to L-Leu, L-Gln, and Phl, the *C*-terminus of Zrv-IIB contains four Aib and three Pro/Hyp residues. The values of $^3J_{N\alpha}$ spin-spin coupling constants for Leu^8, Gln^{11}, and Phl^{16} exceed 6 Hz, and this part of the molecule apparently has the conformation of consecutive turns forming a helix-like structure. The break of sequential connectivities observed on Hyp^{10} (Fig. 1) is attributable to helix bending on Hyp residue; nevertheless, some of the $(i, i + 2)$ and $(i, i + 3)$ contacts pass through this region. That led us to conclude that the helix is not broken on Hyp^{10}. It is well known that the Aib residue is sterically restricted to adopt the helical conformation (Karle and Balaram, 1990), but in contrast to "usual" L-amino acids, it does not possess chirality and can be involved in both right- and left-handed structures. Hence, before the structure calculation we did not exclude the possibility of a left-handed structure in the *C*-terminal part of Zrv-IIB.

The single set of signals in the NMR spectra reveals the absence of *cis-trans* X-Pro peptide bond isomers. The *trans* orientation of the Aib^9-Hyp^{10}, Aib^{12}-Hyp^{13}, and Aib^{14}-Pro^{15} peptide bonds was established based on the intensive sequential NOE crosspeaks between C^{α}-CH_3 protons of Aib and $C^{\delta}H_2$ protons of the subsequent Pro or Hyp residues.

Slow hydrogen-deuterium exchange rates and small temperature coefficients of the chemical shifts of the amide protons over the range of residues from Iva^4 to Phl^{16} indicate reduced solvent accessibility and possible participation in hydrogen bonds. Formation of such bonds along the peptide sequence is consistent with the overall helical structure, although the slow exchange rate of the amide proton of Iva^4 is quite surprising. There are two possible explanations for this: (1) the helix begins from bifurcated hydrogen bond among the NHs of Iva^4, Ile^5, and the carbonyl group of Trp^1 or (2) the *N*-terminal part is completely α-helical and the carbonyl of the acetic group acts as a hydrogen-bond acceptor.

Stereospecific assignments of the Aib residues

One of the most difficult problems in the NMR determination of a peptaibol spatial structure is the stereospecific assignment of the two chemically equivalent but stereochemically different β-methyl groups of Aib residues, which are involved in the majority of the structurally important NOE contacts. The high abundance of Aib residues

TABLE 1 Structural statistics of 20 of the best DYANA structures of zervamicin IIB in DPC micelles

Parameter	Quantity	Unit	DYANA
Target function	average ± s.d.	Å^2	0.014 ± 0.005
Number of distance constraints	NOE		174/29
(upper/lower)	H-bond		30/30
Number of torsion angle	angle ϕ		8
constraints	angle χ^1		3
Upper constraint violations	sum ± s.d.	Å	0.20 ± 0.05
	maximum	Å	0.04
Lower constraint violations	sum ± s.d.	Å	0.0 ± 0.0
	maximum	Å	0.0
Van der Waals constraint	sum ± s.d.	Å	0.20 ± 0.05
violations	maximum	Å	0.04
Angle constraint violations	sum ± s.d.	degrees	0.0 ± 0.0
	maximum	degrees	0.0
rmsd of atom coordinates	backbone	Å	0.20 ± 0.06
residues 1–16)	all heavy atoms	Å	1.24 ± 0.33

in peptaibol sequences makes their assignment critical for structure calculation. Two proposed methods for such assignment are based on the spatial nonequivalence of the methyl groups in the right or left handed helical conformation. The first method uses the values of intraresidual NOE crosspeaks between the amide proton and the two methyl groups (Esposito et al., 1987); in the second method, the up- or low-field shifts of the resonances of $^{13}C^{\beta}$ atoms are used (Anders et al., 1998). However, the results of such an assignment depend completely on the helix handedness, and these methods fail for Aib-rich segments. In this case, full stereospecific assignment can be obtained only on preliminary stages of the structure calculation by using all available data (Anders et al., 2000).

Although the *C*-terminus of Zrv-IIB is clearly not "Aib-rich," (it contains only four nonsequential Aib residues), we attempted to assign Aib methyl groups without any assumption about the helix handedness. This was done by means of the iterative structure calculation (see Materials and Methods). It was found that the *C*-terminus represents a right-handed helix.

Spatial structure of micelle-bound Zrv-IIB

The structure of Zrv-IIB was calculated with the assumption that a single backbone conformation is consistent with all available experimental data. The correctness of this assumption is confirmed by: (1) a small number of constraint violations, (2) small rmsd values (Table 1), and (3) a scatterplot of φ and ψ torsion angles in the obtained set of structures (Fig. 2). The results of the spatial structure calculation are collected in Table 1. The structure of Zrv-IIB (Fig. 3), represents an amphiphilic helix with a total length of 26 Å. The helix is bent on Hyp^{10}, with a bending angle of ~23°. The *N*-terminal part of the molecule forms an α-helix stabilized by five $i + 4 \rightarrow i$-type hydrogen bonds (Ac:CO···HN:Iva^4; Trp^1:CO···HN:Ile^5; Ile^2:CO···HN:

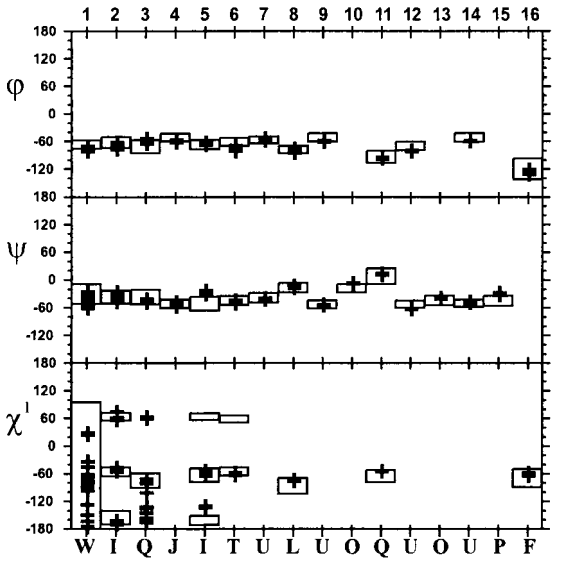

FIGURE 2 Scatter plot of the φ, ψ, χ^1 angles for 20 of the best DYANA structures (after energy minimization) of Zrv-IIB in DPC micelles. The ranges of the corresponding angles for the Zrv-IIB in methanol solution (Balashova et al., 2000) are indicated by the bounding rectangles.

Thr^6; Gln^3:CO···HN:Aib^7; Iva^4:CO···HN:Leu^8). The *C*-terminal half accommodates two hydroxyprolines (Hyp^{10} and Hyp^{13}) and one proline (Pro^{15}) into a helical β-ribbon stabilized by three hydrogen bonds of the $i + 3 \rightarrow i$-type (Thr^6:CO···HN:Aib^9; Leu^8:CO···HN:Gln^{11}; Aib^9:CO···HN:Aib^{12}; an approximate 3_{10}-helix with missing hydrogen bonds at Hyp^{10} and Hyp^{13}) and two hydrogen bonds of the $i + 4 \rightarrow i$-type (Hyp^{10}:CO···HN: Aib^{14}; Aib^{12}: CO···HN: Phl^{16}).

To assess in detail the polarity properties of Zrv-IIB, we calculated the values of MHP on its surface. This potential characterizes the relative hydrophobicity of different parts

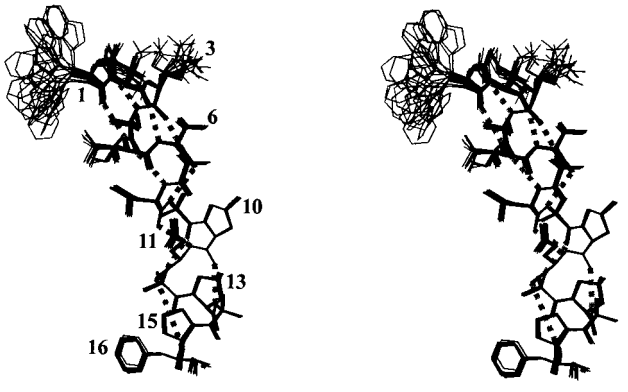

FIGURE 3 Stereoview of 20 of the best DYANA structures (after energy minimization) of Zrv IIB, superimpozed over the backbone atoms of residues 1–16. Only heavy atoms are shown. Hydrogen bonds are shown with gray dotted lines.

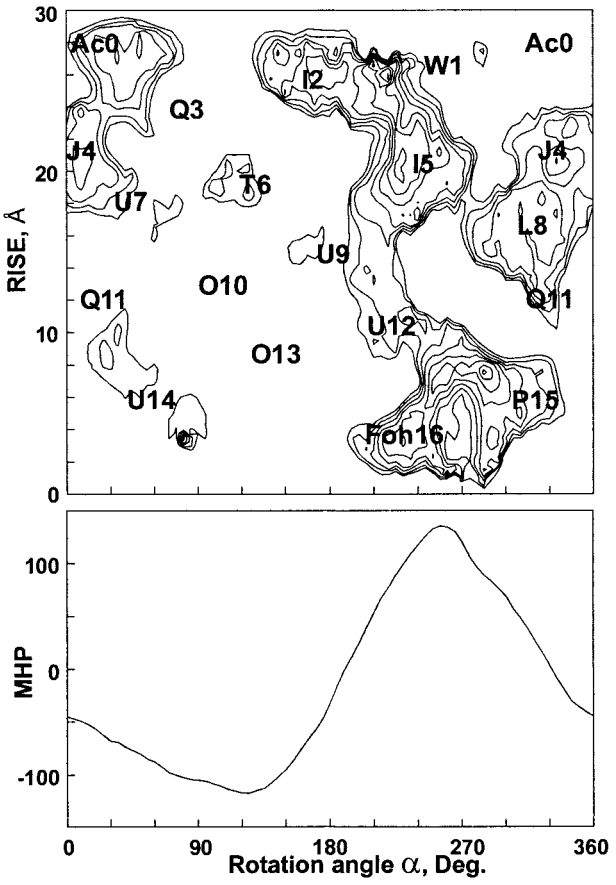

FIGURE 4 Hydrophobic properties of the pore-forming helix of Zrv-IIB. (*Top*), 2-D isopotential map of the MHP on the peptide surface. The value on the *x* axis is the rotation angle about the helix axis; the parameter on *y* axis is the distance along the helix axis. MHP is given in relative numbers. Only the hydrophobic areas with MHP >0.09 are shown. Contour intervals are 0.015. The positions of residues are indicated by letters. (*Bottom*), 1-D MHP plot: angular distribution of MHP created by the peptide atoms on its surface, calculated as described in Efremov and Vergoten (1995).

of the molecular surface. The resulting 2-D isopotential contour map MHP (α, z) is shown in Fig. 4 (*top*). The map is a projection of the surface MHP values onto a cylinder with its z axis corresponding to the helix axis. The rotation angle α is defined around the z axis. Only hydrophobic regions (which have high MHP values) of the Zrv-IIB surface are displayed. It is seen that the helix of Zrv-IIB has a pronounced amphiphilic character. The polar side chains of Gln^3, Thr^6, Hyp^{10}, and Hyp^{13}, along with the small side chains of Aib residues, form a hydrophilic convex side of the molecule. Additionally, the polar face is enhanced by the presence of both the side chain of Gln^{11} and the exposed carbonyl oxygen of Aib^7, which do not participate in intramolecular hydrogen bonds. The ends of the helix are also polar because of the NH and CO groups that are uncompensated by hydrogen bonds. In contrast, the concave surface of the helix is formed by the presence of bulky nonpolar side chains of Trp^1, Ile^2, Ile^5, Leu^8, and Phl^{16} residues. They create a prominent hydrophobic pattern on the peptide surface. It is reasonable to suppose that the polar side chains of the Zrv-IIB molecule line the pore and possibly stabilize the channel bundle via creation of intermolecular hydrogen bonds. Therefore, the side chain mobility in Zrv-IIB bound to membrane-mimic media is of great interest. As illustrated in a scatterplot of the χ^1 torsion angles (Fig. 2), the side chains of Trp^1, Ile^2, Gln^3, and Ile^5 are flexible, whereas Thr^6, Leu^8, Gln^{11}, and Phl^{16} have only one mostly populated χ^1 rotamer (-60 ± 30^o).

Comparison of the backbone and side chain torsion angles of Zrv-IIB in isotropic solvent of moderate polarity (Balashova et al., 2000) and the anisotropic micelle environment (Fig. 2) reveals that the spatial structure of the peptide does not significantly change in these two different media. This conclusion is also confirmed by low backbone rmsd values (0.89 Å) between the two structures. However, the lowest rmsd are observed on the regions 1–9 (0.28 Å) and 11–16 (0.29 Å). So the most significant changes occur near the Hyp^{10}, the site of helix bending. Indeed, the bending angle in DPC (23°) is significantly smaller than that in methanol (47°), thus leading to the increased helix length (26.1 Å vs. 25.6 Å).

Effects of 5- and 16-doxylstearates on the ^{1}H-NMR signals of micelle-bound Zrv-IIB

Relaxation probes are widely used to determine micelle-embedded (Brown et al., 1981; Dubovskii et al., 2001) or water-exposed (Franklin et al., 1994) fragments of polypeptides. To elucidate the location of Zrv-IIB in DPC micelles, the 5- and 16-doxylstearate relaxation probes were incorporated into the DPC micelle with the nitroxide moiety being preferentially located close to the surface and the center of the micelle, respectively (Brown et al., 1981). These probes, in combination, induce broadening of the signals of a peptide immersed in any region of the micelle (Papavoine et al., 1994).

Specific broadening of the proton signals in the Zrv-IIB/DPC complex was monitored using NOESY spectra at the DPC/probe molar ratio of 63:1 (i.e., approximately one relaxation probe per micelle). To characterize the effect of the relaxation probes on the Zrv-IIB protons, we compared the amplitudes of selected intraresidual crosspeaks (Fig. 5) with and without probe. Attenuation of crosspeak intensities induced by 16-doxylstearate (Fig. 5) has a remarkable i, i + 4 and i, i + 3 periodicity. The signals of residues, which form the hydrophobic face of the molecule, were found the most attenuated. In contrast, the signals of the polar residues were almost insensitive to the probe. Addition of 5-doxylstearate decreases the intensities of the crosspeaks, but also with appreciable periodicity (data not shown).

Using the obtained spatial structure of Zrv-IIB, one can construct a model of the Zrv-IIB/DPC complex (Fig. 5,

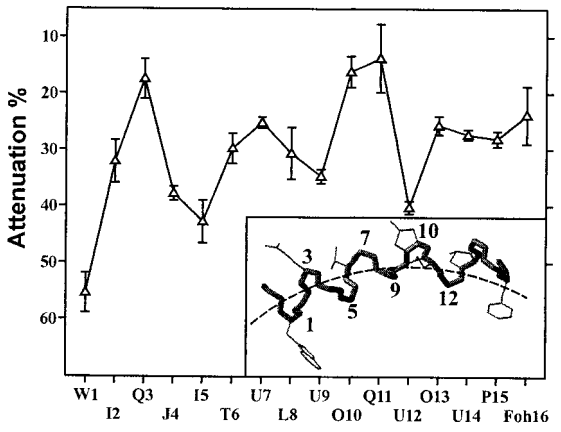

FIGURE 5 Attenuation (%) of intensity of selected crosspeaks (HN/C^{α}-CH_3 (corresponding β protons) for J4, U7, U9, U12, and U14; $C^{\delta}H^1/C^{\delta}H^2$ for O10, O13, and P15; NH/$C^{\alpha}H$ for other residues) in the NOESY τ_m = 100 ms spectra of the Zrv-IIB/DPC complex by the 16-doxylstearate (detergent/stearate ratio 63:1, 30°C, pH 6.8). (*Insert*), Model of the Zrv-IIB/DPC complex; the arc belongs to a circle drawn from the virtual micelle center and has the radius of ~26 Å.

insert). The peptide is oriented approximately parallel to the micelle surface with the polar face directed outside. The strongest attenuation of the signals of Trp^1 corresponds to a deeper immersion of the *N*-terminus, as compared with other parts of the molecule, into the micelle.

DISCUSSION

The spatial structure of Zrv-IIB as compared with other peptaibols

The spatial structure of Zrv-IIB (bent helix) is apparently defined by some essential features in its sequence. α, α-Dialkylated amino acids (Aib, Iva) distributed along the sequence stabilize the helical conformation (Karle and Balaram, 1990), whereas the bend is caused by Pro or Hyp residues. Nowadays, atomic coordinates are published for several peptaibols, such as crystal structures of alamethicin (Alm, 20-residue peptaibol) (Fox and Richards, 1982), Leu^1-zervamicin (Karle et al., 1994), antiamoebin I (16-residue peptaibol highly homologous to Zrv-IIB) (Snook et al., 1998), and NMR structure of chrysospermin C (19-residue peptaibol) in DPC micelles (Anders et al., 2000). All of these structures and Zrv-IIB structures in methanol and DPC represent bent helices, the *N*-termini of the molecules reveal very similar α-helical conformations, whereas their *C*-termini have different spatial structures, from α-helical in chrysospermin C to helical β-ribbon in antiamoebin I and Leu^1-zervamicin. Zrv-IIB has mixed $3_{10}/\alpha_R$ helical conformation in *C*-terminal part. Peptaibol's helices are always bent on a central Pro/Hyp residue (Pro^{14} and Hyp^{10} in Alm and Zrv-IIB, respectively), but the bending angle is different (from 20° in chrysospermin C and Zrv-IIB in DPC environment to 90° in trichorzianin A VII (Condamine et al., 1998)) in various peptides and even in various structures of the same compound. In addition, some of the known structures of peptaibols have exposed carbonyl oxygen at position *i*-3 (Gly^{11} and Aib^7 in case of Alm and Zrv-IIB, respectively), where *i* denotes the bending Pro/Hyp residue. This is because imino acids do not have NH group and, therefore, can not participate in hydrogen bonding. Functional necessity of the helix-bending/carbonyl-exposing Gly^{11}-x-x-Pro^{14} motif was demonstrated on Alm analogs bearing "mutations" in the 11/14 position, which had dramatically decreased the number of conductance levels and their lifetimes (Duclohier et al., 1992; Kaduk et al., 1997, 1998). For zervamicins the significance of the carbonyl exposure in Aib^7 was demonstrated on the "completely apolar" synthetic analog of zervamicin AI. Although exposed backbone carbonyls are the only polar groups in this peptide (Karle et al., 1987), it demonstrates voltage-dependent conductance with two conductance levels (Balaram et al., 1992). Therefore, we can characterize Zrv-IIB in DPC micelles being the norm for the peptaibolic spatial structure.

Structure of Zrv-IIB in the context of the BS model

The BS model is generally used to describe ion channels formed by peptaibols, as confirmed by a great number of experimental evidences. The most convincing arguments include the formation of channels by *N*- or *C*-terminal template-assembled alamethicins (You et al., 1996; Duclohier et al., 1999) and detection of peptaibol pores in membranes by neutron in-plane scattering (He et al., 1996). Recent analysis showed that the antibiotic action of peptaibols is described precisely by the BS model (Beven et al., 1999).

Zrv-IIB has a large content of the 3_{10}-helical structure and the relatively small bending angle, which results in the overall length of ~26 Å. This is significantly longer than a 16-residue β-helix (22.5 Å) and sufficient (taken into account the effect of hydrophobic matching (Killian, 1998)) to span the hydrocarbon region of the bilayer. For example, gramicidin A, another channel-forming peptide, in its active form (helical dimer) has a length ~25.5 Å (Arseniev et al., 1985), easily traverses the bilayer, and if necessary, is able to adjust its thickness (Harroun et al., 1999).

Aromatic residues were found in many TM segments of large, natural ion channels and in gramicidin A (Killian and von Heijne, 2000). In Zrv-IIB such residues (Trp^1 and Phl^{16}) are situated on the edges of the molecule. In a possible TM active state they are capable to stabilize the *N*- and *C*-termini on the interface between hydrocarbon region and the polar headgroups of the lipid bilayer. The exposed carbonyl oxygens in the central part of the molecule are important for the functionality of peptaibols and are also found in structures of nonpeptaibolical ion channels. In a

recently determined structure of the bacterial K^+ channel, the exposed carbonyls play a role of the selective filter (Doyle et al., 1998). In gramicidin A, the exposed carbonyls help to dehydrate monovalent cations passing through the channel (Bechinger, 1999) and form the site of divalent cation binding (Pervushin and Arseniev, 1995). We propose that the exposed carbonyl group in Aib^7 in Zrv-IIB also plays a role in ion conducting.

The strong amphiphilic character of Zrv-IIB helix is pictorially illustrated by the 1-D MHP plot (Fig. 4, *bottom*): a prominent maximum of the function MHP(α) at $210° < \alpha < 330°$ corresponds to its nonpolar side, whereas the minimum at $60° < \alpha < 180°$ to the most hydrophilic one. The hydrophilic face of the helix is represented by the strip of polar residues and ideally suited to the formation of the interior of the pore. On the contrary, the hydrophobic surface pattern most probably corresponds to helix-helix interfaces in the bundle. Analysis of the distribution of hydrophobic and hydrophilic regions on the molecular surface allows speculations about stoichiometry of the Zrv-IIB helix bundle. The distinct minimum and maximum on the 1-D MHP plot (Fig. 4, *bottom*) are characteristic for tetrameric helix bundles. In contrast, pentameric bundles reveal two minima and two maxima on the 1-D MHP plot (Efremov et al., 1999b). These findings are in agreement with the assumption that the low conductance level channels of Zrv-IIB comprise four peptide molecules (Balaram et al., 1992).

The consideration mentioned before makes us confident that Zrv-IIB has sufficient length to span the hydrocarbon region of the membrane and it is well adapted to form an oligomeric, TM ion pore. Earlier, the models for Zrv-IIB bundles were developed based on the crystal structure of Leu^1-zervamicin. In these models, the helices were associated in a parallel fashion, with the *C*-termini situated in close proximity to one another and with the *N*-termini arranged in the funnel shape (Sansom et al., 1993).

The mechanism of Zrv-IIB action

The DPC micelle has a diameter comparable with the membrane thickness and a form of a prolate ellipsoid (Lauterwein et al., 1979). Numerous NMR studies of small helical peptides in micellar environment argue for the retention of their mode of binding (TM or interfacial) upon the transition from bilayer to micelle (Opella et al., 1994; Pervushin and Arseniev, 1995). Thus, our data suggest that monomeric Zrv-IIB binds on the bilayer/water interface in the helical conformation. However, all available experimental data about the pore state of Zrv-IIB are compatible with the BS model. Therefore, an external force is needed to transfer the helix of Zrv-IIB from the interfacial to the TM orientation, because the Zrv-IIB conductance is strongly voltage dependent (Balaram et al., 1992; Kropacheva and Raap, 1999). Thus, Zrv-IIB activation is driven by the interaction of the applied electric field with the helical dipole moment, i.e., reorientation of the amphiphilic helix from interfacial to TM state.

One of the key events in peptaibolic activation is the aggregation of peptides (Woolley et al., 1994). In our NMR study (peptide/detergent ratio 1:40) we have not found evidences for Zrv-IIB aggregation. The electrophysiology investigations of peptaibols are usually conducted at much lower peptide/lipid ratios and, most probably, Zrv-IIB monomeric state remains on the membrane/water interface. Therefore, the aggregation of Zrv-IIB takes place after its transition into the TM orientation.

Zrv-IIB forms channels in the presence of *cis*-positive potentials (Balaram et al., 1992; Kropacheva and Raap, 1999) that, in the context of the voltage-gated insertion model, corresponds to the penetration of its *N*-terminus across the membrane. Such an asymmetrical behavior denotes a higher ability of the *N*-terminus to penetrate hydrocarbon region of the bilayer as compared with the *C*-terminus. It was suggested that insertion of the peptide from the *C*-terminus requires a more extensive, energetically unfavorable dehydration of the polar groups then insertion from the *N*-terminus (Ben-Tal et al., 1996; Chipot and Pohorille, 1998). Estimations with our atomic solvation model (Efremov et al., 1999a) showed that the transfer from water to membrane interior of nonhydrogen-bonded NH or CO group requires +0.8 or +2.0 kcal/mol, respectively. The *N*-terminus of Zrv-IIB has three HN groups, which are not involved in hydrogen bonding, whereas at the proline-rich *C*-terminus there are four uncompensated CO groups. Therefore, insertion from the *N*-terminus of Zrv-IIB is ~5 kcal/mol less energetically costly than that from the *C*-terminus. At the same time, orientation of the Zrv-IIB helix dipole (~41 Debye calculated with CVFF charges) along the external electric field (200 mV applied to a 30-Å thick bilayer) is ~2.6 kcal/mol more favorable than the opposite one (this orientation corresponds to *N*- or *C*-terminal inserted states at a fixed voltage direction). According to these crude estimations, the *N*-terminal insertion into membrane with *cis*-positive potential is significantly more preferable. It is interesting to note that *N*-terminus of Zrv-IIB is more buried in the DPC micelle (Fig. 5) than other parts of the molecule. If this preferential orientation retains on the bilayer membrane, it will promote *N*-terminal penetration across the membrane as well. And we can consider the proposed model of voltage gating as a preorientation/insertion model (Fig. 6). A similar voltage-gating model was proposed for Alm (Barranger-Mathys and Cafiso, 1996).

This work was supported in part by the Ministry of Science and Technology of Russian Federation, by the Russian Foundation of Basic Research

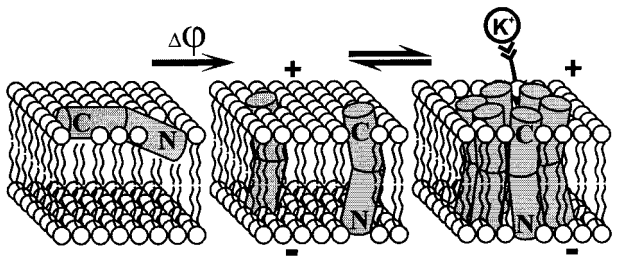

FIGURE 6 Model for Zrv-IIB pore formation. In the absence of a TM potential, monomeric Zrv-IIB molecules are bound in the membrane/water interface. After application of a *cis*-positive potential the *N*-termini of peptides insert into bilayer, the TM molecules aggregate and form pores according to the BS model.

(RFBR) Project 00–15-97877, and by the Netherlands Organization for Scientific Research (NWO) Project 047.006.009.

REFERENCES

Anders, R., O. Ohlenschlager, V. Soskic, H. Wenschuh, B. Heise, and L. R. Brown. 2000. The NMR solution structure of the ion channel peptaibol chrysospermin C bound to dodecylphosphocholine micelles. *Eur. J. Biochem.* 267:1784–1794.

Anders, R., H. Wenschuh, V. Soskic, S. Fischer-Fruhholz, O. Ohlenschlager, K. Dornberger, and L. R. Brown. 1998. A solution NMR study of the selectively 13C, 15N-labeled peptaibol chrysospermin C in methanol. *J. Pept. Res.* 52:34–44.

Argoudelis, A. D., and L. E. Johnson. 1975. United States Patent 3907990.

Argoudelis, A. D., A. Dietz, and L. E. Johnson. 1974. Zervamicins I and II, polypeptide antibiotics produced by *Emericellopsis salmosynnemata*. *J. Antibiot.* 27:321–328.

Arseniev, A. S., I. L. Barsukov, V. F. Bystrov, A. L. Lomize, and Y. Ovchinnikov. 1985. 1H-NMR study of gramicidin A transmembrane ion channel. Head-to-head right-handed, single-stranded helices. *FEBS Lett.* 186:168–174.

Baker, E. N., and R. E. Hubbard. 1984. Hydrogen bonding in globular proteins. *Prog. Biophys. Mol. Biol.* 44:97–179.

Balaram, P., K. Krishna, M. Sukumar, I. R. Mellor, and M. S. Sansom. 1992. The properties of ion channels formed by zervamicins. *Eur. Biophys. J.* 21:117–128.

Balashova, T. A., Z. O. Shenkarev, A. A. Tagaev, T. V. Ovchinnikova, J. Raap, and A. S. Arseniev. 2000. NMR structure of the channel-former zervamicin IIB in isotropic solvents. *FEBS Lett.* 466:333–336.

Barranger-Mathys, M., and D. S. Cafiso. 1996. Membrane structure of voltage-gated channel forming peptides by site-directed spin-labeling. *Biochemistry.* 35:498–505.

Bartels, C., T. Xia, M. Billeter, P. Guntert, and K. Wuthrich. 1995. The program XEASY for computer-supported NMR spectral analysis of biological macromolecules. *J. Biomol. NMR.* 6:1–10.

Baumann, G., and P. Mueller. 1974. A molecular model of membrane excitability. *J. Supramol. Struct.* 2:538–557.

Bax, A., and D. G. Davis. 1985. MLEV-17-based two-dimensional homonuclear magnetization transfer spectroscopy. *J. Magn. Reson.* 65: 355–366.

Bechinger, B. 1999. The structure, dynamics and orientation of antimicrobial peptides in membranes by multidimensional solid-state NMR spectroscopy. *Biochim. Biophys. Acta.* 1462:157–183.

Ben-Tal, N., A. Ben-Shaul, A. Nicholls, and B. Honig. 1996. Free-energy determinants of α-helix insertion into lipid bilayers. *Biophys. J.* 70: 1803–1812.

Beven, L., O. Helluin, G. Molle, H. Duclohier, and H. Wroblewski. 1999. Correlation between anti-bacterial activity and pore sizes of two classes of voltage-dependent channel-forming peptides. *Biochim. Biophys. Acta.* 1421:53–63.

Brown, L. R., C. Bosch, and K. Wuthrich. 1981. Location and orientation relative to the micelle surface for glucagon in mixed micelles with dodecylphosphocholine: EPR and NMR studies. *Biochim. Biophys. Acta.* 642:296–312.

Chipot, C., and A. Pohorille. 1998. Folding and translocation of the undecamer of poly-L-leucine across the water-hexane interface. A molecular dynamics study. *J. Am. Chem. Soc.* 120:11912–11924.

Condamine, E., S. Rebuffat, Y. Prigent, I. Segalas, B. Bodo, and D. Davoust. 1998. Three-dimensional structure of the ion-channel forming peptide trichorzianin TA VII bound to sodium dodecyl sulfate micelles. *Biopolymers.* 46:75–88.

Dauber-Osguthorpe, P., V. A. Roberts, D. J. Osguthorpe, J. Wolff, M. Genest, and A. T. Hagler. 1988. Structure and energetics of ligand binding to proteins: *Escherichia coli* dihydrofolate reductase-trimethoprim, a drug-receptor system. *Proteins.* 4:31–47.

Dementieva, D. V., E. V. Bocharov, and A. S. Arseniev. 1999. Two forms of cytotoxin II (cardiotoxin) from *Naja naja oxiana* in aqueous solution: spatial structures with tightly bound water molecules. *Eur. J. Biochem.* 263:152–162.

Doyle, D. A., C. J. Morais, R. A. Pfuetzner, A. Kuo, J. M. Gulbis, S. L. Cohen, B. T. Chait, and R. MacKinnon. 1998. The structure of the potassium channel: molecular basis of K^+ conduction and selectivity. *Science.* 280:69–77.

Dubovskii, P. V., D. V. Dementieva, E. V. Bocharov, Y. N. Utkin, and A. S. Arseniev. 2001. Membrane binding motif of the P-type cardiotoxin. *J. Mol. Biol.* 305:137–149.

Duclohier, H., K. Kociolek, M. Stasiak, M. T. Leplawy, and G. R. Marshall. 1999. C-terminally shortened alamethicin on templates: influence of the linkers on conductances. *Biochim. Biophys. Acta.* 1420:14–22.

Duclohier, H., G. Molle, J. Y. Dugast, and G. Spach. 1992. Prolines are not essential residues in the "barrel-stave" model for ion channels induced by alamethicin analogues. *Biophys. J.* 63:868–873.

Efremov, R. G., D. E. Nolde, G. Vergoten, and A. S. Arseniev. 1999a. A solvent model for simulations of peptides in bilayers. I. Membrane-promoting α-helix formation. *Biophys. J.* 76:2448–2459.

Efremov, R. G., and G. Vergoten. 1995. Hydrophobic nature of membrane-spanning α-helical peptides as revealed by Monte Carlo simulations and molecular hydrophobicity potential analysis. *J. Phys. Chem.* 99: 10658–10666.

Efremov, R. G., G. Vergoten, and A. S. Arseniev. 1999b. A new "hydrophobic template" method detects segments forming transmembrane α-helical bundles in ion channels. *Theor. Chem. Acc.* 101:73–76.

Epand, R. M., and H. J. Vogel. 1999. Diversity of antimicrobial peptides and their mechanisms of action. *Biochim. Biophys. Acta.* 1462:11–28.

Esposito, G., J. A. Carver, J. Boyd, and I. D. Campbell. 1987. High-resolution 1H NMR study of the solution structure of alamethicin. *Biochemistry.* 26:1043–1050.

Fox, R. O., and F. M. Richards. 1982. A voltage-gated ion channel model inferred from the crystal structure of alamethicin at 1.5-A resolution. *Nature.* 300:325–330.

Franklin, J. C., J. F. Ellena, S. Jayasinghe, L. P. Kelsh, and D. S. Cafiso. 1994. Structure of micelle-associated alamethicin from 1H NMR. Evidence for conformational heterogeneity in a voltage-gated peptide. *Biochemistry.* 33:4036–4045.

Gabay, J. E. 1994. Ubiquitous natural antibiotics. *Science.* 264:373–374.

Gibbs, N., R. B. Sessions, P. B. Williams, and C. E. Dempsey. 1997. Helix bending in alamethicin: molecular dynamics simulations and amide hydrogen exchange in methanol. *Biophys. J.* 72:2490–2495.

Guntert, P., C. Mumenthaler, and K. Wuthrich. 1997. Torsion angle dynamics for NMR structure calculation with the new program DYANA. *J. Mol. Biol.* 273:283–298.

Harroun, T. A., W. T. Heller, T. M. Weiss, L. Yang, and H. W. Huang. 1999. Experimental evidence for hydrophobic matching and membrane-mediated interactions in lipid bilayers containing gramicidin. *Biophys. J.* 76:937–945.

He, K., S. J. Ludtke, D. L. Worcester, and H. W. Huang. 1996. Neutron scattering in the plane of membranes: structure of alamethicin pores. *Biophys. J.* 70:2659–2666.

Henry, G. D., and B. D. Sykes. 1994. Methods to study membrane protein structure in solution. *Methods Enzymol.* 239:515–535.

Jaravine, V. A., D. E. Nolde, M. J. Reibarkh, Y. V. Korolkova, S. A. Kozlov, K. A. Pluzhnikov, E. V. Grishin, and A. S. Arseniev. 1997. Three-dimensional structure of toxin OSK1 from *Orthochirus scrobiculosus* scorpion venom. *Biochemistry.* 36:1223–1232.

Jeener, J., G. N. Meir, P. Bachman, and R. R. Ernst. 1979. Investigation of exchange processes by two-dimensional NMR spectroscopy. *J. Chem. Phys.* 71:4546–4553.

Kaduk, C., M. Dathe, and M. Bienert. 1998. Functional modifications of alamethicin ion channels by substitution of glutamine 7, glycine 11 and proline 14. *Biochim. Biophys. Acta.* 1373:137–146.

Kaduk, C., H. Duclohier, M. Dathe, H. Wenschuh, M. Beyermann, G. Molle, and M. Bienert. 1997. Influence of proline position upon the ion channel activity of alamethicin. *Biophys. J.* 72:2151–2159.

Karle, I. L., and P. Balaram. 1990. Structural characteristics of α-helical peptide molecules containing Aib residues. *Biochemistry.* 29: 6747–6756.

Karle, I. L., J. L. Flippen-Anderson, S. Agarwalla, and P. Balaram. 1994. Conformation of the flexible bent helix of Leu1-zervamicin in crystal C and a possible gating action for ion passage. *Biopolymers.* 34:721–735.

Karle, I. L., J. Flippen-Anderson, M. Sukumar, and P. Balaram. 1987. Conformation of a 16-residue zervamicin IIA analog peptide containing three different structural features: 3(10)-helix, α-helix, and βa-bend ribbon. *Proc. Natl. Acad. Sci. U.S.A.* 84:5087–5091.

Killian, J. A. 1998. Hydrophobic mismatch between proteins and lipids in membranes. *Biochim. Biophys. Acta.* 1376:401–415.

Killian, J. A., and G. von Heijne. 2000. How proteins adapt to a membrane-water interface. *Trends Biochem. Sci.* 25:429–434.

Koradi, R., M. Billeter, and K. Wuthrich. 1996. MOLMOL: a program for display and analysis of macromolecular structures. *J. Mol. Graphics.* 14:51–55.

Kropacheva, T. N., and J. Raap. 1999. Voltage-dependent interaction of the peptaibol antibiotic zervamicin II with phospholipid vesicles. *FEBS Lett.* 460:500–504.

Lauterwein, J., C. Bosch, L. R. Brown, and K. Wuthrich. 1979. Physicochemical studies of the protein-lipid interactions in melittin-containing micelles. *Biochim. Biophys. Acta.* 556:244–264.

Lippens, G., C. Dhalluin, and J. M. Wieruszeski. 1995. Use of a water flip-back pulse in the homonuclear NOESY experiment. *J. Biomol. NMR.* 5:327–331.

Marsh, D. 1996. Peptide models for membrane channels. *Biochem. J.* 315:345–361.

Opella, S. J., Y. Kim, and P. McDonnell. 1994. Experimental nuclear magnetic resonance studies of membrane proteins. *Methods Enzymol.* 239:536–560.

Orekhov, V. Y., D. M. Korzhnev, K. V. Pervushin, E. Hoffmann, and A. S. Arseniev. 1999. Sampling of protein dynamics in nanosecond time scale by 15N NMR relaxation and self-diffusion measurements. *J. Biomol. Struct. Dyn.* 17:157–174.

Papavoine, C. H., R. N. Konings, C. W. Hilbers and F. J. van de Ven. 1994. Location of M13 coat protein in sodium dodecyl sulfate micelles as determined by NMR. *Biochemistry.* 33:12990–12997.

Pervushin, K. V., and A. S. Arseniev. 1995. NMR spectroscopy in the study of the spatial structure of membrane peptides and proteins. *Bioorg. Khim.* 21:83–111.

Piotto, M., V. Saudek, and V. Sklenar. 1992. Gradient-tailored excitation for single-quantum NMR spectroscopy of aqueous solutions. *J. Biomol. NMR.* 2:661–665.

Rance, M., O. W. Sorensen, G. Bodenhausen, C. Wagner, R. R. Ernst, and K. Wuthrich. 1983. Improved spectral resolution in COSY ^{1}H-NMR spectra of protein via double quantum filter. *Biochem. Biophys. Res. Commun.* 117:479–485.

Sansom, M. S. 1991. The biophysics of peptide models of ion channels. *Prog. Biophys. Mol. Biol.* 55:139–235.

Sansom, M. S. 1998. Models and simulations of ion channels and related membrane proteins. *Curr. Opin. Struct. Biol.* 8:237–244.

Sansom, M. S., P. Balaram, and I. L. Karle. 1993. Ion channel formation by zervamicin-IIB. A molecular modelling study. *Eur. Biophys. J.* 21: 369–383.

Snook, C. F., G. A. Woolley, G. Oliva, V. Pattabhi, S. F. Wood, T. L. Blundell, and B. A. Wallace. 1998. The structure and function of antiamoebin I, a proline-rich membrane-active polypeptide. *Structure.* 6:783–792.

States, D. J., R. A. Habercorn, and D. J. Ruben. 1982. 2D NOE with pure absorption phase in four quadrants. *J. Magn. Reson.* 48:286–292.

Szyperski, T., P. Guntert, G. Otting, and K. Wuthrich. 1992. Determination of scalar coupling constants by inverse Fourier transformation of multiplets. *J. Magn. Reson.* 99:552–560.

Vinogradova, O., F. Sonnichsen, and C. R. Sanders. 1998. On choosing a detergent for solution NMR studies of membrane proteins. *J. Biomol. NMR.* 11:381–386.

Woolley, G. A., R. M. Epand, I. D. Kerr, M. S. Sansom, and B. A. Wallace. 1994. Alamethicin pyromellitate: an ion-activated channel-forming peptide. *Biochemistry.* 33:6850–6858.

Wuthrich, K. 1986. NMR of Proteins and Nucleic Acids. John Wiley and Sons, New York.

Yee, A. A., R. Babiuk, and J. D. O'Neil. 1995. The conformation of an alamethicin in methanol by multinuclear NMR spectroscopy and distance geometry/simulated annealing. *Biopolymers.* 36:781–792.

You, S., S. Peng, L. Lien, J. Breed, M. S. Sansom, and G. A. Woolley. 1996. Engineering stabilized ion channels: covalent dimers of alamethicin. *Biochemistry.* 35:6225–6232.